

# A DECOMPOSED CROUZEIX–RAVIART ELEMENT FOR THE FINITE ELEMENT SOLUTION OF THE NAVIER–STOKES EQUATION

F. H. BERTRAND

*CERSIM, Department of Chemical Engineering, Laval University, Québec, QC, Canada, G1K 7P4*

R. E. HAYES

*Department of Chemical Engineering, University of Alberta, Edmonton, AB, Canada, T6G 2G6*

AND

P. A. TANGUY\*

*CERSIM, Department of Chemical Engineering, Laval University, Québec, QC, Canada, G1K 7P4*

## SUMMARY

A methodology for the decomposition of the Crouzeix–Raviart finite element into six linear subelements is described. The resulting element is shown to satisfy the Brezzi–Babuška compatibility condition. The error bounds are also established. A comparison in accuracy between this and the standard Crouzeix–Raviart element is presented for driven cavity flows. Other results include the execution time for the DCR element and the Crouzeix–Raviart element along with both analytical and numerical integration. It is shown that the decomposed element results in shorter execution times with only marginal changes in accuracy.

KEY WORDS Crouzeix–Raviart Analytical integration Brezzi–Babuška condition Navier–Stokes  
Finite element method

## INTRODUCTION

Several specific features characterize the application of the finite element method for incompressible fluid flow problems, namely the treatment of the divergence-free constraint for the imposition of incompressibility and the selection of compatible approximations for the velocity and the pressure. It is well known from variational considerations that the pressure is a Lagrange multiplier for the divergence-free constraint, hence its close relation to the velocity. As a consequence, to ensure reliable computations, the approximation basis of the velocity and the pressure cannot be selected independently but must obey the Brezzi–Babuška compatibility condition.<sup>1</sup> This has given birth to a restricted class of fluid elements.<sup>2</sup> These elements can be divided into two groups, those having a continuous pressure approximation and those having a discontinuous pressure approximation. Only the latter group ensures mass conservation at the element level, because incompressibility is imposed locally.

---

\* Author to whom correspondence should be addressed.

For two-dimensional problems, second-order elements such as the  $Q_2-P_1$  quadrilateral element (biquadratic velocity, discontinuous linear pressure) and the Crouzeix–Raviart triangular element,<sup>3</sup>  $P_2^+-P_1$  (quadratic velocity plus a bubble at the centroid, discontinuous linear pressure) as shown in Figure 1, are among the best elements.

The Crouzeix–Raviart element being triangular, the terms in the Jacobian matrix expressing the geometric transformation from real to reference element are all constant provided that the geometric shape functions are linear (subparametric element). This means that analytical integration can be used, in principle, instead of Gaussian quadrature for the construction of the elementary matrices and vectors, although this may be cumbersome. In contrast, the  $Q_2-P_1$  element has linear terms in the Jacobian, which makes the use of analytical integration impracticable in general.

The objective of this paper is to describe a new element for fluid flow. This element is a decomposed version of the subparametric Crouzeix–Raviart element (subsequently referred to as the decomposed Crouzeix–Raviart or DCR element). In other words, following the idea of Bercovier and Pironneau,<sup>4</sup> we propose to use a different mesh for the approximation of the velocity and the pressure respectively, so that the pattern for the degrees of freedom is the same as that for the classical Crouzeix–Raviart element. This new element retains nearly the same advantages as the original element but enables the use of analytical integration. We give in the following a convergence proof for the DCR element, present the major ideas for its implementation as well as some comparison on timings and accuracy with the parent element in the case of a driven cavity flow.

### MATHEMATICAL FORMULATION

Let us consider the modelling of the creeping flow of a viscous, incompressible fluid in a domain  $\Omega$  with boundary  $\Gamma$  through the following Stokes equations:

$$\operatorname{div} \sigma = f, \quad (1)$$

$$\operatorname{div} v = 0, \quad (2)$$

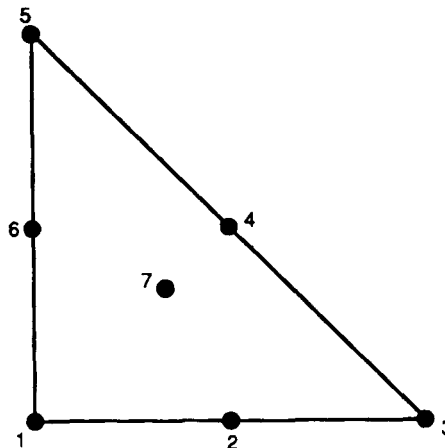


Figure 1. The Crouzeix–Raviart element

where

$$\sigma = -p\delta + 2\mu\dot{\gamma}, \tag{3}$$

$$\gamma = \frac{1}{2}[\text{grad } v + (\text{grad } v)^T]. \tag{4}$$

In these equations,  $v$  is the velocity,  $p$  the pressure,  $f$  a body force,  $\delta$  the unit tensor and  $\mu$  the viscosity. If we take  $v \in [H_0^1(\Omega)]^2$  and  $p \in L_0^2(\Omega)$  with  $L_0^2(\Omega) = \{q \in L^2(\Omega); \int_{\Omega} q \, dx = 0\}$ , then the resolution of this problem is equivalent to considering the following min-max problem:

$$\min_{v \in [H_0^1(\Omega)]^2} \max_{p \in L_0^2(\Omega)} \frac{1}{2} \int_{\Omega} \mu [\dot{\gamma}(v)]^2 \, d\Omega - \int_{\Omega} p \, \text{div } v \, d\Omega - \int_{\Omega} f v \, d\Omega. \tag{5}$$

This leads to the following weak problem:

$$a(v, \psi) - b(\psi, p) = (f, \psi), \quad \forall \psi \in [H_0^1(\Omega)]^2, \tag{6}$$

$$b(v, \Phi) = 0, \quad \forall \Phi \in L_0^2(\Omega), \tag{7}$$

where

$$a(v, \psi) = \mu \int_{\Omega} \text{grad } v \, \text{grad } \psi \, d\Omega, \tag{8}$$

$$b(v, \Phi) = \int_{\Omega} \Phi \, \text{div } v \, d\Omega \tag{9}$$

and where  $(\cdot, \cdot)$  stands for the standard scalar product in  $L^2(\Omega)$ , i.e.

$$(u, v) = \int_{\Omega} uv \, d\Omega. \tag{10}$$

The discretization is carried out using the finite element method. The following discrete formulation (Uzawa algorithm) is then readily obtained:

$$A_r V^{i+1} - B^T P^i = F, \tag{11}$$

$$A_r = A + r B^T B, \tag{12}$$

$$P^{i+1} = P^i - r B V^{i+1}, \tag{13}$$

where  $V^{i+1}$  and  $P^{i+1}$  denote respectively the velocity and pressure vectors at Uzawa iteration  $i + 1$ .  $A$ ,  $B$  and  $F$  stand respectively for the diffusion matrix, the divergence matrix and the body force vector. Finally,  $r$  is the penalty parameter ( $r \gg 1$ ).

### THE DCR ELEMENT

#### Presentation

Consider the Crouzeix-Raviart element in Figure 1. Let us now subdivide this element, simply by connecting the node at the centroid to each of the other six nodes in turn. This results in six linear microelements of equal area,  $T_i$  ( $i = 1, 2, \dots, 6$ ), as shown in Figure 2. We keep the degrees of freedom in pressure at the centroid of the macroelement.

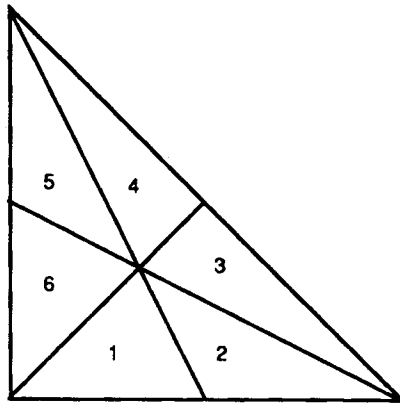


Figure 2. The DCR element

*Theoretical properties*

Let us begin by introducing the following vector spaces:

$$V_h = \{v_h \in [C^0(\Omega)]^2; v_h|_T \in [P_2^+(T)]^2, \forall T \in \tau_h; v_h|_\Gamma = 0\}, \tag{14}$$

$$V_h^* = \{v_h \in [C^0(\Omega)]^2; v_h|_{T_i} \in [P_1(T_i)]^2; \forall i = 1, \dots, 6, \forall T \in \tau_h, T = \cup_{i=1,6} T_i; v_h|_\Gamma = 0\}, \tag{15}$$

$$Q_h = \{q_h \in L_0^2(\Omega); q_h|_T \in P_1(T), \forall T \in \tau_h\}, \tag{16}$$

$$W_h^* = \{v_h \in V_h^*; b(v_h, q_h) = 0, \forall q_h \in Q_h\}, \tag{17}$$

where  $P_2^+(T) = P_2(T) \oplus \lambda_1 \lambda_2 \lambda_3$  in area co-ordinates and where  $\tau_h$  stands for a regular family of finite elements (for more details of this and the following proof, see e.g. Reference 5 or 6). It follows, therefore, that using  $V_h^*$  as the discrete space for the velocity field means approximating the quadratic shape functions of the Crouzeix–Raviart element by piecewise linear shape functions that we denote by  $\{\phi_i\}_{i=1,7}$ . We may now state an approximation result.

*Theorem*

(i) There exists a constant  $\alpha > 0$  independent of  $h$  such that

$$a(v_h, v_h) \geq \alpha \|v_h\|_{1,\Omega}^2, \quad \forall v_h \in W_h^*. \tag{18}$$

(ii) There exists a constant  $\beta > 0$  independent of  $h$  such that

$$\sup_{v_h \in V_h^*} \frac{b(v_h, q_h)}{\|v_h\|_{1,\Omega}} > \beta \|q_h\|_{0,\Omega}, \quad \forall q_h \in Q_h, \tag{19}$$

or equivalently (hereafter referred to as the discrete Brezzi–Babuška condition)

$$\inf_{q_h \in Q_h} \sup_{v_h \in V_h^*} \frac{b(v_h, q_h)}{\|v_h\|_{1,\Omega} \|q_h\|_{0,\Omega}} \geq \beta. \tag{20}$$

*Proof.* (i) We have  $a(v, v) \geq \alpha \|v\|_{1,\Omega}^2, \forall v \in [H^1(\Omega)]^2$ . The result follows from  $V_h^* \subset [H^1(\Omega)]^2$ .

(ii) We first recall a lemma which implies the Brezzi–Babuška condition with  $\beta$  independent of  $h$ .

*Lemma*

Let us denote by  $X_h$  and  $M_h$  discrete approximations of  $[H_0^1(\Omega)]^2$  and  $L_0^2(\Omega)$ . Let us assume that there exists a linear continuous operator  $\pi_h: [H_0^1(\Omega)]^2 \rightarrow X_h$  and a constant  $c > 0$  independent of  $h$  such that  $\forall v \in [H_0^1(\Omega)]^2$ ,

$$\int_{\Omega} q_h \operatorname{div}(v - \pi_h v) \, d\Omega = 0, \quad \forall q_h \in M_h, \tag{21}$$

$$\|\pi_h v\|_{1,\Omega} < c \|v\|_{1,\Omega}. \tag{22}$$

Then the discrete Brezzi–Babuška condition (16) holds with  $\beta$  independent of  $h$ .

It is now clear that to prove (ii) it is sufficient to build such an operator for  $X_h = V_h^*$  and  $M_h = Q_h$ . Consequently, for every triangle  $T \in \tau_h$  with vertices  $a_i, 1 \leq i \leq 3$ , we uniquely define  $\pi_h v|_T \in V_h^*$  by

$$\pi_h v|_T(a_i) = v(a_i), \quad 1 \leq i \leq 3, \tag{23}$$

$$\int_{[a_i, a_j]} (\pi_h v|_T - v) \, ds = 0, \quad 1 \leq i \leq 3, \quad 1 \leq j \leq 3, \tag{24}$$

$$\int_T x_k \operatorname{div}(\pi_h v|_T - v) \, d\Omega = 0, \quad k = 1, 2, \quad x = (x_1, x_2). \tag{25}$$

Such an operator complies with the lemma. The remainder of the proof is analogous to the one for the construction of  $\pi_h$  in the case of the Crouzeix–Raviart element.

The theorem implies that the Stokes problem has a unique solution  $(u_h, p_h) \in V_h^* \times Q_h$  and that

$$\|u_h - v\|_{1,\Omega} + \|p_h - p\|_{0,\Omega} \leq c \left( \inf_{v_h \in V_h^*} \|v_h - v\|_{1,\Omega} + \inf_{q_h \in Q_h} \|q_h - p\|_{0,\Omega} \right), \tag{26}$$

with  $c$  independent of  $h$ . Moreover, if  $\tau_h$  is uniformly regular and  $\Omega$  is convex, it follows from the theory of Lagrangian interpolation in  $\mathbb{R}^2$  that if  $(v, p) \in [H^2(\Omega) \cap H_0^1(\Omega)]^2 \times [H^1(\Omega) \cap L_0^2(\Omega)]$ , then

$$\|u_h - v\|_{1,\Omega} + \|p_h - p\|_{0,\Omega} \leq ch(\|v\|_{2,\Omega} + \|p\|_{1,\Omega}). \tag{27}$$

*Implementation*

The implementation of this element follows closely that of the Crouzeix–Raviart element. The major difference is the addition of the steps to partition the macroelement and the subassembly of the microelements back into the macroelement.

The computation of the integral terms in the variational formulation, when performed on the microelements, gives rise to six  $6 \times 6$  microelementary matrices, which must be subassembled in the correct fashion to yield the macroelementary  $14 \times 14$  matrix, which in turn is assembled into the global matrix (a similar operation is performed for the residual).

Each microelement is an isoparametric  $P_1$  element. Therefore the Jacobian of the geometric transformation, which we denote  $J_i$ , and the velocity gradients are constant within each microelement. Consequently, analytical integration of the terms that appear in equations (11)–(13) is straightforward. For example, denoting  $\phi_k$  and  $\phi_k$ ,  $k = 1, \dots, 3$ , the shape functions on real element  $T_i$  and the reference element respectively, it can be readily seen that analytical integration

of the diffusion term

$$\int_{T_i} (\partial\phi_k/\partial x_m)(\partial\phi_l/\partial x_m) dx, \quad 1 \leq k, \quad l \leq 3, \quad 1 \leq m \leq 2, \quad (28)$$

over microelement  $T_i$ ,  $i = 1, \dots, 6$ , reduces to

$$\det |J_i| (\partial\phi_k/\partial x_m)(\partial\phi_l/\partial x_m) \text{ area}(T_i). \quad (29)$$

*Remark 1*

Analytical integration is still possible in the case of the full Navier–Stokes equations. More precisely, the linearized inertial terms as they appear in the Newton–Raphson scheme break down into a sum of integrals that can be handled analytically.

*Remark 2*

Thus far we have implicitly considered the context of Cartesian co-ordinates. The resolution of problems in axisymmetric co-ordinates by means of analytical integration is a little more complex owing to the presence of the radius in the underlying formulation, which must be expressed in terms of the nodal co-ordinates prior to integration. Nevertheless, this is again relatively straightforward and will not be presented here.

## RESULTS AND DISCUSSION

There are two important factors to consider when examining a prospective element, namely the accuracy of the solution and the amount of execution time required to achieve it. Accordingly, we considered as a test problem the classical driven cavity, for which no analytical solution exists. The domain and boundary conditions are shown in Figure 3. Let us take as a reference solution

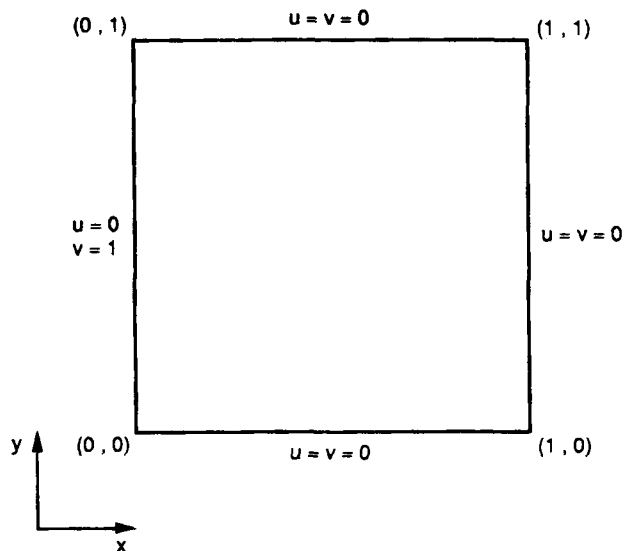


Figure 3. Solution domain and boundary conditions for the driven cavity

$(v_{ref}, p_{ref})$  the one obtained for the finest  $P_2$ -mesh ( $h=0.05$ , 894 elements). The discretization errors  $\|v - v_{ref}\|_{0,\Omega}$  and  $\|p - p_{ref}\|_{0,\Omega}$  versus the mesh size  $h$  are given in Figures 4 and 5 respectively. We can see from these two plots that for the meshes used, both elements achieve essentially the same level of accuracy.

The second point to consider is the amount of computer time required to solve a given problem. For this test we again used the driven cavity problem. Tests were conducted on four different mesh sizes, using an Apollo DN 3000 workstation running UNIX under SR 9.5. For comparison purposes we used a six-point quadrature formula and also analytical integration on the Crouzeix-Raviart element.

We consider first the execution time requirements for each of the cases, for the resolution of the Stokes equations. Timings are given for matrix construction, residual construction and overall solution time for the first and second iterations. Figure 6 shows the execution time required for the construction of the elementary matrices as a function of the number of elements. We see that the construction of the matrix for the DCR element using analytic integration requires about 40% of the time required for Gaussian quadrature on the Crouzeix-Raviart element. The gain is only marginal when the Crouzeix-Raviart element is used in conjunction with analytical integration. We have plotted in Figure 7 the timing for the residual construction. Here the trends are quite different. The DCR element requires about 65% of the execution time of the Crouzeix-Raviart element with numerical integration, while the gain is still more important when one uses analytical integration for the parent element. This may appear surprising at first.

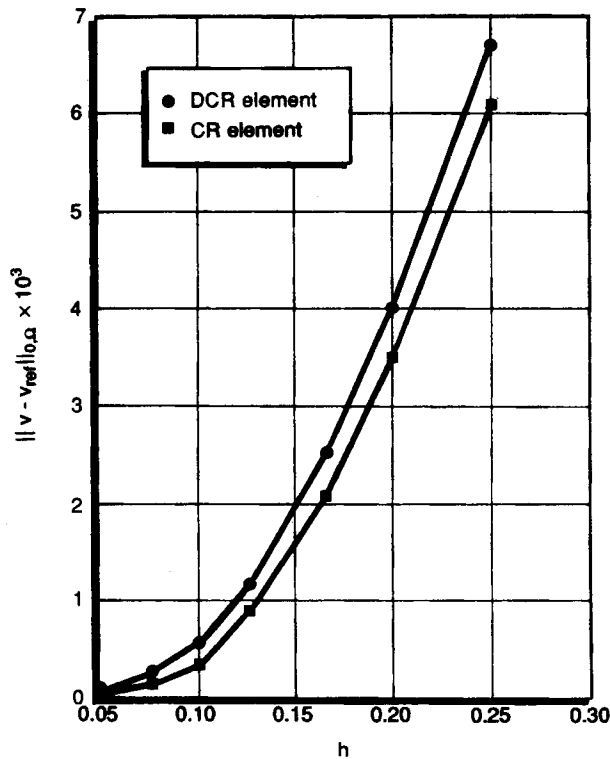


Figure 4. Graph of  $\|v - v_{ref}\|_{0,\Omega} \times 10^3$  versus  $h$

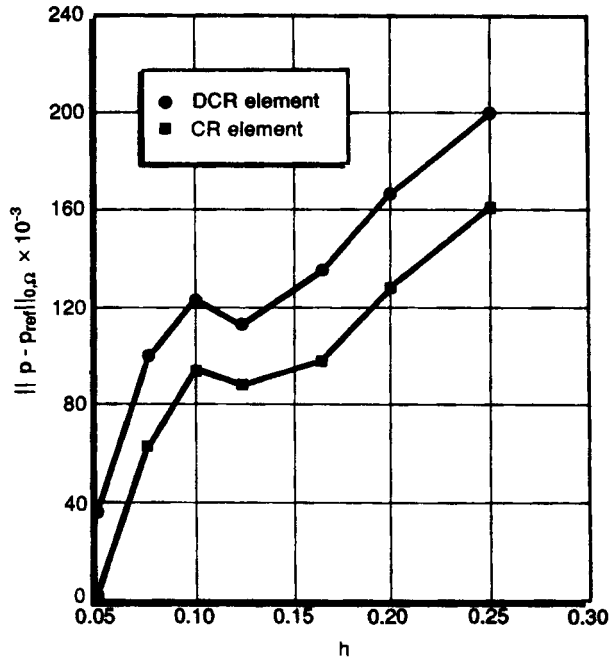


Figure 5. Graph of  $\|p - p_{ref}\|_{0,\Omega} \times 10^{-3}$  versus  $h$

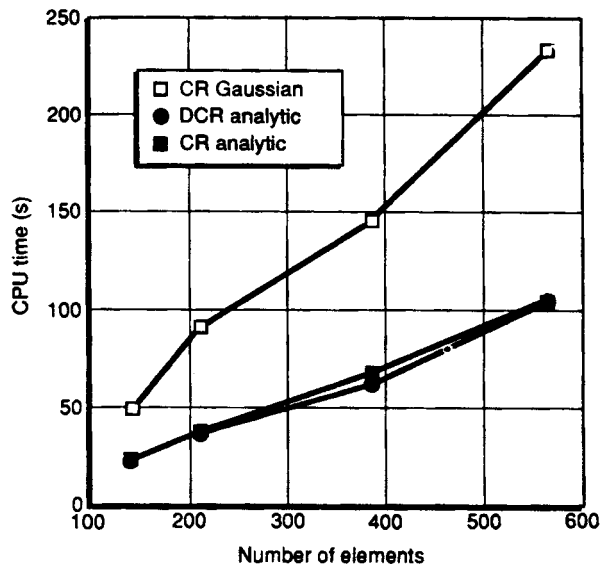


Figure 6. Comparison of the execution time required to build the global matrix as a function of the number of elements for the two elements, including analytical and numerical integration schemes for the Crouzeix-Raviart element



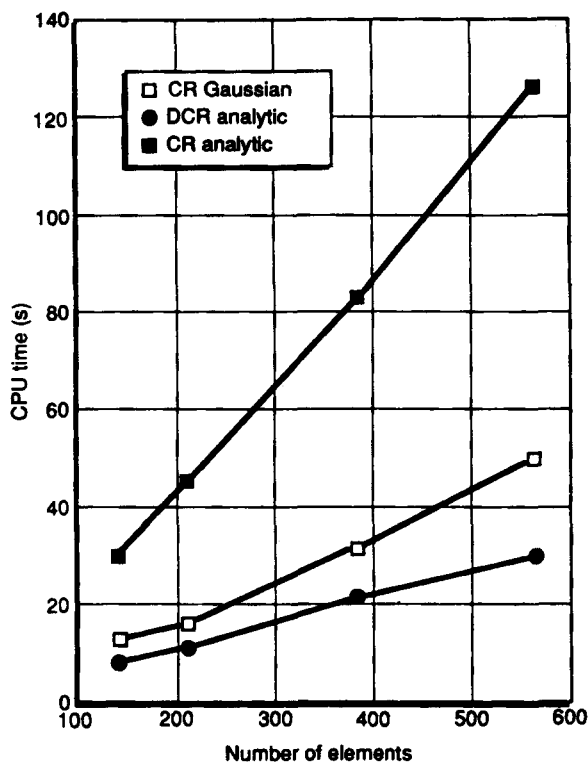


Figure 7. Execution time required to build the residual as a function of the number of elements for the two elements, including analytical and numerical integration schemes for the Crouzeix–Raviart element

When using analytical integration with the  $P_2^+ - P_1$  element, however, one intermediate step necessary to build the residual is to build the matrix; indeed the matrix is used as a multiplier of the former nodal solutions in the construction process. This results in a quite dramatic increase of the computational cost.

To put these numbers into the context of the overall solution time required to solve the problem, we show in Figure 8 the total execution time as a function of the problem size for a complete iterative step. For the size of problems considered here, savings in overall execution time amount to roughly 20%, irrespective of the integration method used with the original Crouzeix–Raviart element. We believe that the gain in performance on a vector computer for very large problems might be much higher, since the factoring cost is proportionally less important in the overall execution time (the factoring is more vectorizable), although this point was not investigated.

In Figure 9 we have displayed the timing results for two iterations, the first one for which both the matrix and the residual are built and the second one for which only the residual is built. Such results are typical of those obtained with a modified Newton–Raphson method or for any problem in which the matrix is fixed in the iterative process, for instance as in the use of the augmented Lagrangian method<sup>7</sup> for non-Newtonian fluid flow. Again it can be seen that the gain is about 20% as in Figure 8 when the DCR element is used.

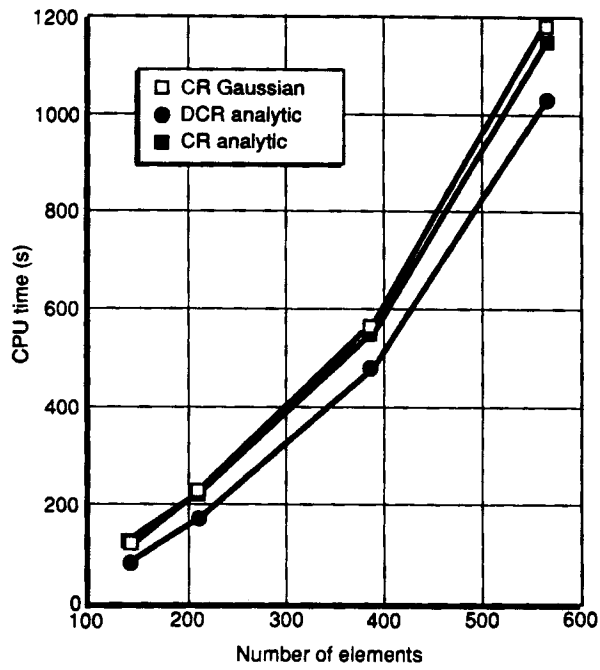


Figure 8. Total execution time required for one problem iteration

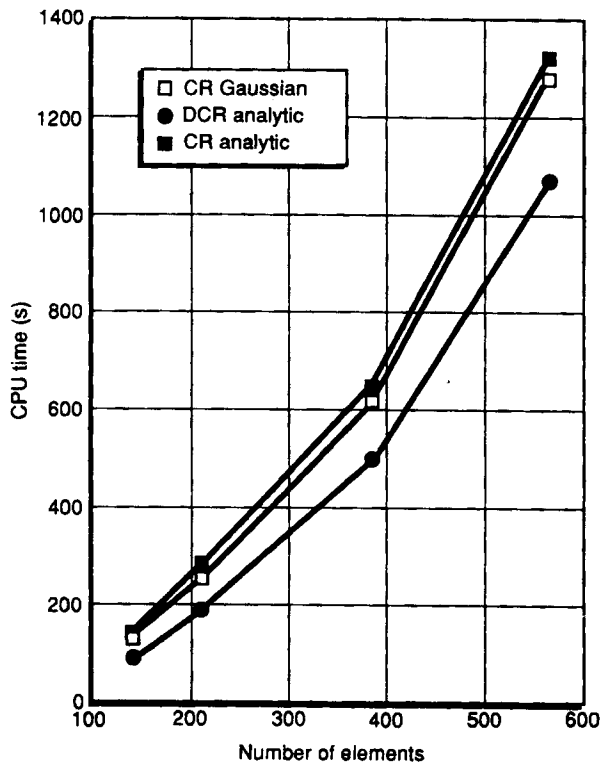


Figure 9. Total execution time required for two problem iterations

## CONCLUDING REMARKS

A new element based on a decomposition of the subparametric Crouzeix–Raviart element into six linear triangles has been presented. We have seen that the DCR element combined with analytic integration can offer significant savings in execution time over the use of the Crouzeix–Raviart element with Gaussian quadrature or even analytic integration, without significant loss in accuracy. Furthermore, its implementation in a standard finite element programme is straightforward. In view of the increasing size of problems being solved by the finite element method, we believe that this element can be useful to many FEM practitioners.

## ACKNOWLEDGEMENT

This work was funded by the Natural Science and Engineering Research Council of Canada.

## REFERENCES

1. F. Brezzi, 'On the existence, uniqueness and approximation of saddle-point problems arising from Lagrangian multipliers', *RAIRO, Sér. Anal. Numér.*, **8**, 129 (1974).
2. M. Fortin, 'Old and new elements for incompressible flows', *Int. j. numer. methods fluids*, **1**, 347 (1981).
3. M. Crouzeix and P. A. Raviart, 'Conforming and non-conforming finite element methods for solving the stationary Stokes equation', *RAIRO, Sér. Anal. Numér.*, **7**, 33 (1973).
4. M. Bercovier and O. Pironneau, 'Error estimates for the finite element method solution of the Stokes problem in primitive variables', *Numer. Math.*, **33**, 211 (1977).
5. P. A. Raviart and J. M. Thomas, *Introduction à l'Analyse Numérique des Equations aux Dérivées Partielles*, Masson, Paris, 1983.
6. V. Girault and P. A. Raviart, *Finite Element Approximation of the Navier–Stokes Equations*, Springer, Berlin, 1981.
7. P. Tanguy, M. Fortin and L. Choplin, 'Finite element simulation of dip coating, II: Non-Newtonian fluids', *Int. j. numer. methods fluids*, **4**, 459–475 (1984).